Nonharmonic oscillations of nanosized cantilevers due to quantum-size effects

Martin Olsen,* Per Gradin, Ulf Lindefelt, and Håkan Olin†
Department of Natural Sciences, Engineering and Mathematics, Mid Sweden University, SE-851 70 Sundsvall, Sweden
(Received 26 June 2009; revised manuscript received 26 January 2010; published 16 February 2010)

Using a one-dimensional jellium model and standard beam theory we calculate the spring constant of a vibrating nanowire cantilever. By using the asymptotic energy eigenvalues of the standing electron waves over the nanometer-sized cross-section area, the change in the grand canonical potential is calculated and hence the force and the spring constant. As the wire is bent more electron states fits in its cross section. This has an impact on the spring "constant" which oscillates slightly with the bending of the wire. In this way we obtain an amplitude-dependent resonance frequency of the oscillations that should be detectable.

DOI: 10.1103/PhysRevB.81.054304 PACS number(s): 62.23.Hj, 62.25.−g, 62.30.+d

I. INTRODUCTION

Nanoelectromechanical (NEMS) systems are usually still in the macroscopic regime in the sense that quantum effects do not play a large role. This is due to the smallness of the quantum energy of a mechanical structure even if it is of nanometer dimensions. For example, $\hbar\omega$ for a cantilever with a large resonance frequency of 1 GHz will only have an energy of 4 μeV, which is much smaller than the thermal energy at normal conditions. The corresponding amplitude A of such quantum oscillations, given by $\frac{1}{2}kA^2=\hbar\omega$, where k is the transverse spring constant, will be very low and hard to detect.[1] However, in certain circumstances quantum-size effects have a significant effect.[2] For example, Stafford *et al.*[3] and others[4–6] calculated the tensile force in a nanowire during its elongation. They found jumps in the force corresponding to different numbers of electron states that fits in the wires cross section when the wire was stretched. This effect has been measured.[7,8] The canonical component in NEMS is the cantilever, which is used in a large number of systems including atomic force microscopes and cantilever-based sensors. It is not obvious that bending a cantilever will give the same effect as in the Stafford system where the diameter of the nanowire could be reduced to a fraction.

Here, we show that quantum-size effects should be included for thin cantilevers, and even if the effect is small, at resonance the effect will be detectable due the high accuracy at which frequency of oscillation can be measured: down to tenth of millihertz.[9] We use the same kind of free-electron model as in earlier studies to calculate the spring constant of the cantilever.

II. MODEL

When a nanowire is bent the length of a fiber on the upper side of the wire increases, corresponding to reduction in the width of the cross section. Conversely the length is reduced on the lower part corresponding to an increase in the width of the cross section. In the middle is an unaffected neutral line. This effects will change the cross-sectional area of the nanowire which, in turn, change the tensile force in the wire as it becomes more bent. Because the wire is assumed to be thin, only a few wave modes under the Fermi level fits in the cross section. We use a one-dimensional density of states in a similar way as in earlier works.[3–6] We consider a straight nanowire, which we bend by applying a perpendicular force at the free end. The other end of the wire is attached to bulk material letting electrons flow in and out of the wire. By using standard beam theory we find that bending of the wire yields an increase in the cross-section area. The wire has the length L and a quadratic cross section with undeformed side d_0, see Fig. 1. When we applying a perpendicular force F at the end of the cantilever at $x=L$, we obtain

$$M = F(L-x), \tag{1}$$

$$\sigma_x = \frac{M}{I}z, \tag{2}$$

$$\sigma_y = \sigma_z = 0, \tag{3}$$

where M is the moment of the force F at position x, I is the areal moment of inertia of the cross–section, and σ_x, σ_y, and σ_z are stresses in the x, y, and z directions, respectively. For strains in the x, y, and z directions we have

$$\varepsilon_x = \frac{\sigma_x}{E}, \tag{4}$$

$$\varepsilon_y = -\nu\varepsilon_x, \tag{5}$$

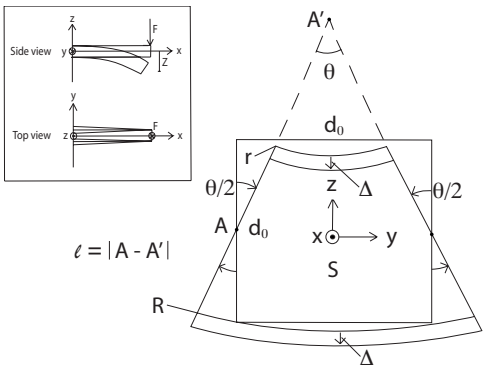

FIG. 1. A cross section S of the cantilever before and after a perpendicular force is applied on the wires end. Inset: side view and top view of the cantilever nanowire. The expansions and contractions of the cross sections are larger nearer the fixed end if the cross section can contract and expand freely.

$$\varepsilon_z = -\nu\varepsilon_x, \tag{6}$$

where ν is the Poisson's ratio and E is the Young's modulus. This lead to the deformation of the cantilever cross section as shown in Fig. 1.

For the deformations u_y we have

$$\varepsilon_y = \frac{\partial u_y}{\partial y} \Rightarrow \tag{7}$$

$$u_y = -\frac{\nu F}{EI}(L-x)yz + H(x,z), \tag{8}$$

using partial integration, where $H(x,z) \equiv 0$ by symmetry. For the deformations u_z we have

$$\varepsilon_z = \frac{\partial u_z}{\partial z} \Rightarrow \tag{9}$$

$$u_z = -\frac{\nu F}{2EI}(L-x)z^2 + G(x,y). \tag{10}$$

The shear strain γ_{yz} is assumed to be zero, so

$$\gamma_{yz} = \frac{\partial u_y}{\partial z} + \frac{\partial u_z}{\partial y} = 0, \tag{11}$$

yielding an expression for $G(x,y)$ to use in Eq. (10). We finally obtain

$$u_y = -\frac{\nu F}{EI}(L-x)yz, \tag{12}$$

$$u_z = -\frac{\nu F}{2EI}(L-x)(z^2 - y^2) + f(x), \tag{13}$$

where $f(x)$ is the engineering beam theory solution describing the bending of the neutral line $y=z=0$ which only implies a translation of the whole cross section and therefore can be left out when calculating its deformation.

When the wire is deformed by the force, the side of the cross section is bent inwards with an angle $\theta/2$ on the upper part of the wire cross section and is bent outwards with the same angle on the lower side. On the top side there is a compression of the wire and on the down side there is an elongation. The area after the deformation is the difference between two circle sectors with radii R and r, respectively, and θ is the top angle

$$S = \pi(R^2 - r^2)\frac{\theta}{2\pi}, \tag{14}$$

$$R = \ell + \frac{d_0}{2} + \Delta, \tag{15}$$

$$r = \ell - \frac{d_0}{2} + \Delta, \tag{16}$$

$$\sin\left(\frac{\theta}{2}\right) = \frac{d_0}{2\ell}, \tag{17}$$

resulting in $S \approx d_0^2(1+\Delta/\ell)$. From Eq. (13) we see that

$$\Delta = \frac{\nu F}{2EI}(L-x)\left(\frac{d_0}{2}\right)^2. \tag{18}$$

The radius of curvature ℓ is given by

$$\frac{1}{\ell} \approx \left|\frac{\partial^2 u_z}{\partial y^2}\right| = \frac{\nu F}{EI}(L-x). \tag{19}$$

We then obtain, using Eqs. (18) and (19),

$$S = d_0^2\left[1 + \frac{1}{8}\left(\frac{\nu F(L-x)d_0}{EI}\right)^2\right]. \tag{20}$$

A beam of length L with a perpendicular force F applied at the end bends a distance Z

$$Z = \frac{FL^3}{3EI} = \frac{kZL^3}{3EI}, \tag{21}$$

where $F=kZ$, and k, in turn, is the transverse spring constant of the wire. We then obtain

$$S = d_0^2\left[1 + \frac{9\nu^2 d_0^2 (L-x)^2 Z^2}{8L^6}\right], \tag{22}$$

which is independent of the Young's modulus E. The eigenenergies for the standing electron waves that fits the cross section is in the limit of large eigenvalues[10]

$$E_n = \frac{\hbar^2}{2m}\frac{4\pi}{S}n, \tag{23}$$

where n is the quantum number and m the electron mass. The grand canonical potential of the electron gas in the nanowire is for low temperature given by[3,6]

$$\Omega = -\sum_n \int_0^L \frac{4}{3}\sqrt{\frac{2m}{\pi^2\hbar^2}}[E_F - E_n(x)]^{3/2}dx. \tag{24}$$

Integration of Eq. (24) using Eq. (22) for *small* bending Z yielded

$$\Omega = -\sum_n \sqrt{\frac{2m}{\pi^2\hbar^2}}\left[\frac{4}{3}(E_F - E_{n0})^{3/2}L + \frac{2}{3}\sqrt{E_F - E_{n0}}E_{n0}\frac{9}{8}\left(\frac{d_0\nu}{L^3}\right)^2 Z^2 L^3\right], \tag{25}$$

which is Blom *et al.*[6] plus a term proportional to the down bending Z squared. We have

$$E_{n0} = \frac{\hbar^2}{2m}\frac{4\pi}{d_0^2}n = E_0 n, \tag{26}$$

$$N = \frac{E_F}{E_0}, \tag{27}$$

where N, if rounded off down to an integer, is the number of energy levels below Fermi level. Using, for example, $d_0=4$

nanometer and $E_F=5.5$ eV (gold, silver) we obtain the number of energy levels below Fermi level $N=183$. $d_0=1$ nm yields $N=11$. The force F which is assumed to be due to the electron gas is given by $F=-\frac{\partial\Omega}{\partial Z}=kZ$, so we obtain, assuming $\frac{\partial L}{\partial Z}=0$ (no elongation of the wire), the spring constant

$$k_0=\sum_{n=1}^{N}\frac{3d_0^2\nu^2}{2L^3}\sqrt{\frac{2m}{\pi^2\hbar^2}}\sqrt{E_F-E_{n0}}E_{n0}. \tag{28}$$

Disregarding the variation in S with x in Eq. (22) and assuming the same deformation in every cross section as at the fixed end to simplify the integration we obtain

$$S=d_0^2\left[1+\frac{9\nu^2d_0^2Z^2}{8L^4}\right]. \tag{29}$$

Using Eq. (29) in Eq. (24) and taking the derivative yielded

$$k=\sum_{n=1}^{N}\sqrt{E_F-\frac{E_0n}{1+\frac{9\nu^2d_0^2Z^2}{8L^4}}}\frac{\sqrt{\frac{2m}{\pi^2\hbar^2}}nE_0\frac{18d_0^2\nu^2}{4L^3}}{\left[1+\frac{9\nu^2d_0^2Z^2}{8L^4}\right]^2}, \tag{30}$$

where

$$N=\frac{E_F}{E_0}\left(1+\frac{9\nu^2d_0^2Z^2}{8L^4}\right). \tag{31}$$

Because Eq. (30) should yield the same as Eq. (28) for small bending, Eq. (30) should be corrected with factor 1/3 to account for the variation in S with x

$$k=\sum_{n=1}^{N}\sqrt{E_F-\frac{E_0n}{1+\frac{9\nu^2d_0^2Z^2}{8L^4}}}\frac{\sqrt{\frac{2m}{\pi^2\hbar^2}}nE_0\frac{6d_0^2\nu^2}{4L^3}}{\left[1+\frac{9\nu^2d_0^2Z^2}{8L^4}\right]^2} \tag{32}$$

This expression is valid for *arbitrary* bending Z. Plotting k from Eq. (32) as a function of Z is shown in Fig. 2. Replacing a sum by an integral we found

$$\sum_{n=1}^{N}n\sqrt{N-n}\approx\frac{4}{15}(N^{5/2}-N). \tag{33}$$

Using Eq. (28) for *small* bending and Eq. (33), neglecting the second term in the rhs of Eq. (33) because $N>1$, we obtain the spring constant for the unbent wire

$$k_0=\frac{\sqrt{2}\nu^2}{5\pi^2}\sqrt{\frac{d_0^2m^3E_F^5}{\hbar^6}}\left(\frac{d_0}{L}\right)^3, \tag{34}$$

due to an increase in the electron gas density of states that fits in the nanowire when bent. The k axis always intersect the curve at a local maxima or minima of the k values, as we see in Fig. 2. We may therefore have $k=k_0+\text{const}\times Z^2$ for not too large bending, see Eq. (39).

III. DISCUSSION

We may then rewrite the harmonic equation with a bending-dependent spring constant

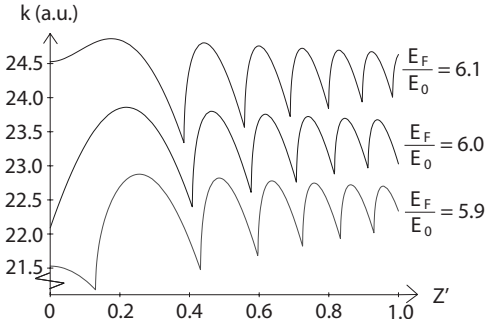

FIG. 2. Example of spring constant k variation as a function of bending $Z'=\sqrt{\frac{9}{8}}\frac{\nu d_0 Z}{L^2}$ obtained from an equation having the same type of dependency on n and Z as Eq. (32) has, i.e., Eq. (38). The three curves show the forms of the curve obtained from Eq. (38) for $\frac{E_F}{E_0}$ below, at and above an integer. We see that Eq. (38) is independent of the sign of Z as is to be expected by symmetry. The k axis always intersects the curve at a local maxima or minima. However, this maxima or minima may not be very wide depending on how close we are that a new electron state will fit when bending the wire slightly. We see in the figure that the width is small when $\frac{E_F}{E_0}$ is close to an integer (middle curve) and broader farther from an integer.

$$\frac{d^2Z}{dt^2}+\omega_0^2Z+\beta Z^3+2\gamma\frac{dZ}{dt}=F\sin(\omega t). \tag{35}$$

This is called the Duffing equation. The amplitude A and phase ϕ of the stationary solution to the linear ($\beta=0$) differential equation is given by

$$A=\frac{F}{\sqrt{(\omega_0^2-\omega^2)^2+(2\omega\gamma)^2}}, \tag{36}$$

$$\tan\phi=-\frac{2\omega\gamma}{\omega_0^2-\omega^2}. \tag{37}$$

Because of the weak nonlinearity the resonance frequency is shifted from ω_0 to $\sqrt{\omega_0^2+\frac{3}{4}\beta A^2}$, see Ref. 11. We then obtain a shift in the amplitude maximum toward a higher frequency for positive β, as shown in Fig. 3. Because frequency can be measured at high precision, even small changes can be experimentally detected. The oscillation in the weakly nonlinear case takes place around the same point of equilibrium as in the low amplitude, i.e., linear harmonic case.

We see from Fig. 2 that β is positive for the upper curve and negative for the lower curve around $Z=0$. The middle curve is problematic: very close to E_F/E_0 being an integer we have $k=k_0+\text{const}\times|Z|$. This discontinuity in the first derivative of the curve at $Z=0$ vanishes however quickly when we move away from $E_F/E_0=\text{integer}$.

The results in this paper should be valid for wires with small enough diameter so that the one-dimensional distribution function is a good approximation. From the result presented, it should be possible to experimentally determine how close we are to that a new state would fit in the nanowire. By first measuring the low-amplitude frequency of the oscillating nanowire and then increase the amplitude it should be possible to determine if the resonance frequency is

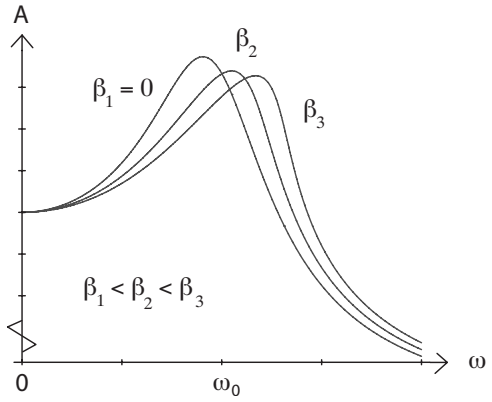

FIG. 3. The amplitude response of a driven weakly nonlinear harmonic oscillator. $\beta=0$ corresponds to the harmonic case where the resonance frequency is ω_0. When the amplitude is increased (or β is increased), the resonance frequency is shifted toward higher values for positive β and toward lower values for negative β, from ω_0 to $\sqrt{\omega_0^2+\frac{3}{4}\beta A^2}$.

increased or decreased corresponding to positive or negative β. To illustrate the changes in Eq. (32) with different values of $N=E_F/E_0$ we made plots. The function to be plotted is

$$k'(Z) = \sum_{n=1}^{N(1+CZ^2)} \sqrt{N - \frac{n}{1+CZ^2}} \times \frac{n}{(1+CZ^2)^2}, \quad (38)$$

where $C=\frac{9\nu^2 d_0^2}{8L^4}$, which has the same type of dependency on n and Z as Eq. (32) has. We then obtain curves as in Fig. 2. The lowest curve is obtained for $N=5.9$, the middle curve for $N=6.0$ and the upper curve for $N=6.1$. For small bending Z, Eq. (38) becomes

$$k'(Z) = \sum_{n=1}^{N} n\sqrt{N-n} + CZ^2 \sum_{n=1}^{N} \left(\frac{5n^2 - 4Nn}{2\sqrt{N-n}} \right) + \cdots. \quad (39)$$

Dividing Eq. (38) with the first term in Eq. (39) yields the relative size of the effect of bending on the spring constant. A typical value of the relative change in spring constant due to bending was about 0.01–0.1 % up to $N=200$ at $\sqrt{\frac{9}{8}}\frac{\nu d_0 Z}{L^2}=0.05$. At high N we would need a smaller deflection Z to reach the local maximum and minimum points in the curve in Fig. 2, however, the relative change tends to be smaller as N is increased. From Eqs. (39) and (35) we can calculate $\beta/(C\omega_0^2)$ in Eq. (35). This yields

$$\xi = \frac{\beta}{C\omega_0^2} = \frac{\sum_{n=1}^{N} \left(\frac{5n^2 - 4Nn}{2\sqrt{N-n}} \right)}{\sum_{n=1}^{N} n\sqrt{N-n}}. \quad (40)$$

A plot of Eq. (40) is shown in Fig. 4.

What effect has a finite temperature on this result? Following Blom *et al.*[6] we have the grand canonical potential $\Omega=E_{tot}-\mu N_{tot}$ where the chemical potential $\mu \approx E_F$ at room temperature and

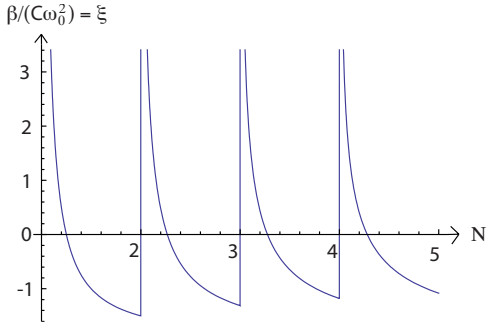

FIG. 4. (Color online) $\beta/(C\omega_0^2)$ as a function of $N=\frac{E_F}{E_0}$ obtained by dividing the second term in Eq. (39) with the first term and identifying the spring constant in Eq. (35). $C=\frac{9\nu^2 d_0^2}{8L^4}$. We note the singularities at integer numbers, corresponding to when we have $k=k_0+\text{const}\times|Z|$ instead of $k=k_0+\text{const}\times Z^2$, which is the normal behavior near $Z=0$.

$$N_{tot} = \sum_n \int_{E_n}^{\infty} g(E-E_n) f(E) dE, \quad (41)$$

$$E_{tot} = \sum_n \int_{E_n}^{\infty} g(E-E_n) f(E) E dE, \quad (42)$$

where $g(E)$ is the one-dimensional density of states, $f(E)$ is the Fermi-Dirac distribution function, and E_n is the energy of the state n that fits the cross section. Using $F=-\frac{\partial\Omega}{\partial Z}=kZ$ and Eq. (32) we argue that the generalized expression for the spring constant k valid for any temperature should be given by

$$k = \sum_{n=1}^{N'} \left\{ \frac{\sqrt{\frac{2m}{\pi^2\hbar^2}} n E_0 \frac{6d_0^2\nu^2}{4L^3}}{\left[1+\frac{9\nu^2 d_0^2 Z^2}{8L^4}\right]^2} \times \int_{E_n'}^{E_{cut}} \frac{1/2}{\sqrt{E - \frac{E_0 n}{1+\frac{9\nu^2 d_0^2 Z^2}{8L^4}}}} \frac{dE}{(e^{(E-\mu)/k_B T}+1)} \right\}, \quad (43)$$

where

$$N' = \frac{E_{cut}}{E_0}\left(1+\frac{9\nu^2 d_0^2 Z^2}{8L^4}\right), \quad (44)$$

$$E_n' = \frac{E_0 n}{\left(1+\frac{9\nu^2 d_0^2 Z^2}{8L^4}\right)}, \quad (45)$$

and the upper integration limit $E_{cut}\to\infty$. Equation (43) reduces to Eq. (32) when $T\to 0$. A plot of Eq. (43) for different temperature is shown in Fig. 5.

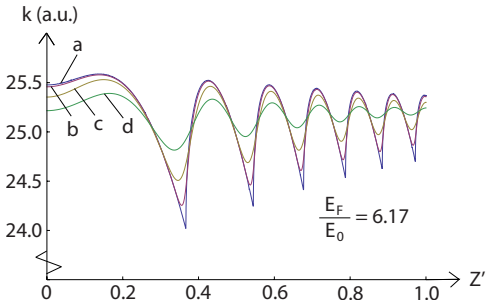

FIG. 5. (Color online) Example of spring constant as a function of different bending $Z' = \sqrt{\frac{9}{8}}\frac{\nu d_0 Z}{L^2}$ for four different temperatures using Eq. (43). Curve a: k_BT=0.0001 eV, curve b: k_BT=0.01 eV, curve c: k_BT=0.025 eV (room temperature), and curve d: k_BT =0.05 eV. The plot is made using μ=2.9 eV, E_0=0.47 eV (i.e., d_0=1 nm), and the upper energy limit of integration is taken to be E_{cut}=5.0 eV. Increasing E_{cut} to 7.0 yields no visible change in the curves. For $E_{cut} > \mu$ the contribution to the expression decreases rapidly due to the Fermi-Dirac function.

Due to temperature, more states becomes available for the electrons from E_F up to about $E_F + k_BT$ and decreasing the number of available states between E_F and about $E_F - k_BT$. This effect tend to make the transition at integer numbers in Fig. 4 (where a new energy level is added) less sharp, smoothing the spikes in $\xi = \beta/(C\omega_0^2)$. We also see in Fig. 5 that at room temperature the curve follows the zero temperature curve well, except around the minima where a new state is added due to bending. The room-temperature curves here becomes smoothed. The condition that temperature is not important *other than close to N* being an integer must be that $k_BT \ll E_0$, where E_0 is the difference in energy between two energy levels. Using Eq. (26) we obtain this condition as

$$\frac{k_BT}{E_0} = \frac{k_BTmd_0^2}{2\pi\hbar^2} \ll 1. \tag{46}$$

To obtain agreement between the curve for finite temperature and the zero-temperature curve around Z=0 we need Eq. (46) to be fulfilled. Room temperature corresponds to $\frac{k_BT}{E_0}$ =5.3% in Fig. 5. This means that even for a diameter of 1 nm the system needs to be cooled[12] if one is to use the zero-temperature result. However, interesting results can also be obtained at room temperature, as we see in the curves in Fig. 5.

Experimentally, a way to detect these amplitude-dependent resonance frequencies might be *in situ* transmission electron microscopy probing where one can see the wire while manipulating it.[13,14] For the thermal vibration of a nanowire we have $\frac{1}{2}k_0A^2 = k_BT$. For weak nanowires this amplitude is relatively large at room temperature and can be observed.[15] If one choose to drive the oscillation with an external electric field this effect must be taken into account. Small metallic nanosized cantilever has been manufactured.[16–18]

IV. CONCLUSIONS

Using a one-dimensional jellium model and standard beam theory we calculate the spring constant of a vibrating

TABLE I. Table of different L=40-nm-long gold nanowires (ν=0.44) that may be used to measure the predicted effects. The maximum temperature T of the wire and its diameter d_0 are coupled by Eq. (46), if one wants to use the zero-temperature result. However, as seen in Fig. 5 the modification of the curves due to temperature are rather small at room temperature and interesting measurements on the system can also be made at this higher temperature. ξ varies periodically with increasing $N = \frac{E_F}{E_0}$ and is obtained from Eq. (40) for the zero-temperature case. Small changes in d_0 (yielding E_0) can result in large changes in ξ if N is close to an integer. At about 25–30 % of the distance between N being integers ξ becomes zero as it change sign from positive to negative. The frequency shift is proportional to the square of the amplitude A. In the table we use A=12 nm, that is 30% of the wires length L. For the thermal vibration of a nanowire we have $\frac{1}{2}k_0A^2 = k_BT$. Using this equation for the weakest nanowire in the table this amplitude becomes 13 nm at room temperature.

d_0 (nm)	T (K)	$M(\times 10^{-22})$ (kg)	k_0 (mN/m)	ξ	f_0 (MHz)	Δf (kHz)
1.0	55[a]	1.93[b]	0.0469[c]	−0.344 [d]	39.2[e]	−0.992 [f]
1.5	25[a]	4.34[b]	0.238[c]	−0.464 [d]	58.9[e]	−4.52 [f]
2.0	14[a]	7.72[b]	0.750[c]	−0.395 [d]	78.4[e]	−9.12 [f]
2.5	8.8[a]	12.1[b]	1.83[c]	−0.281 [d]	97.8[e]	−12.6 [f]
3.0	6.2[a]	17.4[b]	3.80[c]	−0.107 [d]	118[e]	−8.35 [f]
3.5	4.5[a]	23.6[b]	7.05[c]	−0.200 [d]	138[e]	−24.7 [f]
4.0	3.4[a]	30.1[b]	12.0[c]	−0.198 [d]	159[e]	−37.0 [f]

[a]From Eq. (46) using $\frac{k_BT}{E_0}$=1% and d_0 in the table.
[b]The mass of the wire $M = \rho L d_0^2$, where ρ is the density.
[c]Calculated using Eq. (34) and the data in the table.
[d]Calculated using Eq. (40) and the data in the table.
[e]From $f_0 = \frac{1}{2\pi}\sqrt{\frac{k_0}{M}}$ using k_0 and M in the table.
[f]From Eq. (47) using the data in the table. A=12 nm.

nanowire cantilever. By using the asymptotic energy eigenvalues of the standing electron waves over the nanometer-sized cross-section area, the change in the grand canonical potential is calculated and hence the force and the spring constant. As the wire is bent more electron states fits in its cross section. This has an impact on the spring "constant" which oscillates slightly with the bending of the wire. In this way we obtain an amplitude-dependent resonance frequency of the oscillations that should be detectable. Because the weak nonlinearity the resonance frequency is shifted from ω_0 to $\sqrt{\omega_0^2+\frac{3}{4}\beta A^2}$. Using Eq. (40) we can replace β with $\xi C\omega_0^2$. We then obtain from this the relative frequency shift

$$\frac{\Delta\omega}{\omega_0} \approx \frac{27}{64}\xi\nu^2\left(\frac{d_0}{L}\right)^2\left(\frac{A}{L}\right)^2, \tag{47}$$

where A is the amplitude of the oscillation and $\omega=2\pi f$. The data of some wires possible to use in an experiment is shown in Table I.

*martin.olsen@miun.se
†hakan.olin@miun.se

[1] M. Blencowe, Phys. Rep. **395**, 159 (2004).
[2] N. Agraït, A. L. Yeyati, and J. M. van Ruitenbeek, Phys. Rep. **377**, 81 (2003).
[3] C. A. Stafford, D. Baeriswyl, and J. Bürki, Phys. Rev. Lett. **79**, 2863 (1997).
[4] J. M. van Ruitenbeek, M. H. Devoret, D. Esteve, and C. Urbina, Phys. Rev. B **56**, 12566 (1997).
[5] C. Yannouleas and U. Landman, J. Phys. Chem. B **101**, 5780 (1997).
[6] S. Blom, H. Olin, J. L. Costa-Krämer, N. Garcia, M. Jonson, P. A. Serena, and R. I. Shekhter, Phys. Rev. B **57**, 8830 (1998).
[7] G. Rubio, N. Agrait, and S. Vieira, Phys. Rev. Lett. **76**, 2302 (1996).
[8] A. Stalder and U. Dürig, Appl. Phys. Lett. **68**, 637 (1996).
[9] F. J. Giessibl, Rev. Mod. Phys. **75**, 949 (2003).
[10] W. A. Strauss, *Partial Differential Equations: An Introduction* (Wiley, New York, 1992).
[11] A. H. Nayfeh and D. T. Mook, *Nonlinear Oscillations, Pure and Applied Mathematics* (Wiley, New York, 1979).
[12] P. Mohanty, D. A. Harrington, K. L. Ekinci, Y. T. Yang, M. J. Murphy, and M. L. Roukes, Phys. Rev. B **66**, 085416 (2002).
[13] P. Poncharal, Z. L. Wang, D. Ugarte, and W. A. de Heer, Science **283**, 1513 (1999).
[14] K. Svensson, Y. Jompol, H. Olin, and E. Olsson, Rev. Sci. Instrum. **74**, 4945 (2003).
[15] M. M. J. Treacy, T. W. Ebbesen, and J. M. Gibson, Nature (London) **381**, 678 (1996).
[16] Z. Lee, C. Ophus, L. M. Fischer, N. Nelson-Fitzpatrick, K. L. Westra, S. Evoy, V. Radmilovic, U. Dahmen, and D. Mitlin, Nanotechnology **17**, 3063 (2006).
[17] E. Luber, R. Mohammadi, C. Ophus, Z. Lee, N. Nelson-Fitzpatrick, K. Westra, S. Evoy, U. Dahmen, V. Radmilovic, and D. Mitlin, Nanotechnology **19**, 125705 (2008).
[18] S. G. Nilsson, X. Borrisé, and L. Montelius, Appl. Phys. Lett. **85**, 3555 (2004).